

SWIFT X-RAY OBSERVATIONS OF CLASSICAL NOVAE

J.-U. NESS¹, G.J. SCHWARZ², A. RETTER³, S. STARRFIELD¹, J.H.M.M. SCHMITT⁴, N. GEHRELS⁵, D. BURROWS⁶, J.P. OSBORNE⁷

(Dated: accepted by ApJ (March 8, 2007)*)
Draft version November 30, 2018

ABSTRACT

The new γ -ray burst (GRB) mission *Swift* has obtained pointed observations of several classical novae in outburst. We analyzed all the observations of classical novae from the *Swift* archive up to 30 June, 2006. We analyzed usable observations of 12 classical novae and found 4 non-detections, 3 weak sources and 5 strong sources. This includes detections of 2 novae exhibiting spectra resembling those of Super Soft X-ray binary Source spectra (SSS) implying ongoing nuclear burning on the white dwarf surface. With these new *Swift* data, we add to the growing statistics of the X-ray duration and characteristics of classical novae.

Subject headings: stars: individual (V574 Pup, V382 Nor, V1663 Aql, V5116 Sgr, V1047 Cen, V476 Sct, V477 Sct, LMC 2005, V1494 Aql, V4743 Sgr, V1188 Sco) — stars: novae — X-rays: stars

1. INTRODUCTION

The explosions of Classical Novae (CNe) occur in close binary star systems where mass is accreted onto a white dwarf (WD) from a low-mass secondary star. The accreted material gradually becomes degenerate, and when temperatures become high enough and the pressure at the bottom of the accreted envelope exceeds a certain value, a thermonuclear runaway results. Enough energy is deposited in the accreted material to eject some fraction from the WD. The outburst can last several months to years, and CNe become active in X-rays at some time during their outburst (e.g., Pietsch et al. 2005; Pietsch et al. 2006). The relatively slow evolution makes CNe ideal targets for *Swift*, as no accurate times of observation need to be scheduled and they can be observed with great flexibility.

The evolution of X-ray emission starts soon after outburst when the expanding nova envelope is still small and dense. The energy peak during this earliest time, called the “fireball” phase (Shore et al. 1994; Schwarz et al. 2001), is expected to occur at X-ray wavelengths. This phase is extremely difficult to observe since it is predicted to last only a few hours after the beginning of the outburst so that it is over before the nova can be discovered in the optical. As the envelope increases in size and cools, the opacity increases, shifting the radiation towards wavelengths longer than the hydrogen absorp-

tion edge at 13.6 eV (911 Å). The expanding, cooling envelope gives rise to the large and rapid increase in the visual luminosity of the nova. Around the time of visual maximum, X-rays from the underlying WD are trapped inside the large column density of the ejecta. However, shocks may develop within the early expanding ejecta producing a hard, sub-Eddington luminosity, X-ray spectral energy distribution (e.g., V382 Vel, Orío et al. 2001a; Mukai & Ishida 2001). As the shell continues to expand, the density and opacity drop, and X-rays emitted from the surface of the WD eventually become visible (Krautter et al. 1996). Soft X-ray emission originates from hot layers produced by the nuclear burning of the remaining accreted material on the WD. This material burns in equilibrium at a high but constant luminosity, $\propto L_{\text{Eddington}}$ (Gallagher & Starrfield 1978). The spectral energy distribution resembles that of the super-soft X-ray sources (SSS), (e.g. Cal 83, Paerels et al. 2001; Lanz et al. 2005).

Recent observations of novae during this phase show that the flux can also be highly variable on short timescales (see, e.g. Ness et al. 2003; Osborne et al. 2006). The duration of this SSS phase is predicted to be inversely proportional to the WD mass (Starrfield 1991), but a review of the ROSAT X-ray sky survey (Orío et al. 2001b) showed that the timescale is much shorter than predicted, implying either that the masses of WDs in CNe are much higher than commonly assumed, or that the X-ray turn-off is a function of more than the WD mass. A different approach was proposed by Greiner et al. (2003) who found from the available data that systems with shorter orbital periods display long durations of supersoft X-ray phases, while long-period systems show very short or no SSS phase at all. They speculate that shorter periods may be related to a higher mass transfer rate (e.g., by increased irradiation) and thus to the amount of material accreted before the explosion.

Another source of X-ray emission from novae are emission lines from material that has been radiatively ionized. These lines are expected to be present during

¹ School of Earth and Space Exploration, Arizona State University, Tempe, AZ 85287-1404, USA: Jan-Uwe.Ness,sumner.starrfield@asu.edu

² Department of Geology & Astronomy, West Chester University, 750 S. Church Street, West Chester, PA 19383, USA

³ Department of Astronomy and Astrophysics, Penn State University, 525 Davey Lab, University Park, PA, 16802-6305, USA

⁴ Hamburger Sternwarte, Gojenbergsweg 112, 21029 Hamburg, Germany

⁵ NASA/Goddard Space Flight Center, Greenbelt, Maryland 20771, USA

⁶ Department of Astronomy and Astrophysics, Penn State University, University Park, Pennsylvania 16802, USA

⁷ Department of Physics & Astronomy, University of Leicester, Leicester, LE1 7RH, UK

*This version contains additional material

the entire evolution, but are usually only observed once the nuclear fuel is consumed and the bright continuous SSS spectrum (that outshines the emission lines) fades. The ejecta quickly recombine until a collisional equilibrium is reached. This equilibrium reflects the kinetic temperature distribution of the plasma and the elemental abundances can be derived (Ness et al. 2005). This phase is called the nebular phase, and is also seen at other wavelengths (Shore et al. 2003). In some cases, X-ray emission from lines has been observed earlier, either prior to the SSS phase, superimposed on the SSS spectrum (*e.g.*, V1494 Aql), or during times of extreme variability when the SSS emission suddenly declines before recovery (*e.g.*, V4743 Sgr, Ness et al. 2003).

X-ray observations provide important clues to the properties and dynamics of novae. The evolution of the SSS depends on the WD mass, the mass loss rate (via radiatively driven winds or common envelope mass loss), the amount of ejected material, the amount of material remaining on the WD, the binary separation, and the expansion velocity of the ejecta. Analysis of the X-ray emission can also provide insight into the composition of the ejecta. Unfortunately, only a few novae have been studied extensively in X-rays with much of the recent information coming from *Chandra* and *XMM-Newton*. Now, with *Swift*, we have the possibility of studying novae in large numbers in order to assess statistical properties. *Swift* also allows for coordination of higher-resolution observations with *Chandra* and *XMM-Newton* since it has always been difficult to predict the brightness in X-rays and to estimate the optimal exposure time for X-ray observations with the gratings.

In this paper we discuss the *Swift* XRT instrument briefly in Sect. 2.1. Since interstellar absorption plays an important role in Galactic novae, we discuss the expected effects on the detection of SSS in Sect. 2.2. In Sect. 3 we sort the observations by non-detections, detections of weak sources, and strong sources based on our extraction statistics detailed out in the appendix section A.2. We discuss our results in Sect. 4 and expand on the type of X-ray emission that was detected in the *Swift* observations. Finally, Appendix A.1 provides background information for each nova.

2. *Swift* OBSERVATIONS

2.1. The instrument

Our entire dataset has been obtained with the X-ray Telescope (XRT) aboard *Swift* (Burrows et al. 2005). The XRT instrument is a CCD detector behind a Wolter Type I grazing incidence mirror consisting of 12 nested shells. The field of view covers $23.6' \times 23.6'$, imaged on a detector with 600×600 pixels, thus each pixel corresponds to $2.36''$. The point spread function (PSF) can be parameterized, and source radii of 10 pixels and 5 pixels include 80.5 percent and 60.5 percent of the total energy, respectively (Moretti et al. 2004). The positional accuracy is $2.5''$, or one pixel. The energy range covers 0.2 – 10 keV with the Full Width at Half Maximum (FWHM) energy resolution varying from ~ 50 eV at 0.1 keV to ~ 190 eV at 10 keV. In Fig. 1 we show a comparison of effective areas of *Swift*, *Chandra*, and *XMM-Newton*. In general, the *Swift* XRT has a smaller

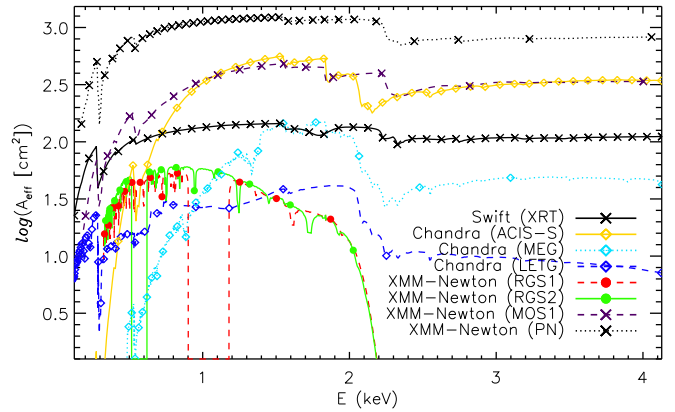


FIG. 1.— Comparison of XRT effective areas of *Swift* with other X-ray instruments that are sensitive in the same spectral region. None of the *Chandra* or *XMM-Newton* gratings has a higher effective area than the XRT. The CCD detectors: ACIS-S (*Chandra*) and EPIC (PN/MOS1; *XMM-Newton*) have higher effective areas. The spectral resolution of the XRT is similar to either the ACIS or EPIC detectors, but the spectral resolution of the gratings is much superior.

effective area than the *Chandra*/ACIS-S except at low energies (long wavelengths) where the *Chandra* ACIS-S suffers from large calibration uncertainties. The EPIC detectors PN and MOS1 (*XMM-Newton*) have 50 percent and 20 percent higher effective areas, respectively. The XRT, ACIS, and EPIC instruments have similar spectral resolution. The XRT effective area is larger than that of the gratings aboard *Chandra* (LETG and MEG) and *XMM-Newton* (RGS1 and RGS2), but the XRT spectral resolution is much lower. Fig. 1 demonstrates that the XRT is an ideal instrument for exploring the emission level of novae using reasonable exposure times ($\sim 3 - 6$ ksec). Once a nova is detected with *Swift* and found sufficiently bright, additional observations can be requested with the high-resolution grating instruments aboard *Chandra* and *XMM-Newton* to obtain detailed spectral information. The detector was operated in Photon Counting (PC) mode which provides 2D imaging, spectral information, and 2.5-sec time resolution.

2.2. Observability of the Super Soft Source phase in Classical Novae

Unfortunately, many Galactic CNe have large extinction which has a pronounced effect on the observability of the SSS emission. To illustrate this we attenuate a series of *Cloudy* models (Ferland et al. 1998) through different amounts of H I column densities and determine the resulting *Swift* counts. The models use non-LTE atmospheres by Rauch (1997) for planetary nebula nuclei with effective temperatures in the range of $(1 - 6) \times 10^5$ K (8–50 eV) as the input source. The model luminosity was fixed at 10^{38} erg sec $^{-1}$, which is approximately the Eddington luminosity for a $1-M_{\odot}$ star. The spectral energy distributions were attenuated by H I column densities ranging from $1 - 20 \times 10^{21}$ cm $^{-2}$ and then converted to *Swift* net count rates using the effective area of the XRT and scaled to a 1 ksec exposure at 1 kpc. The logarithms of the expected total XRT counts are shown as contours in Fig. 2. As expected, the ability to detect a SSS is highly dependent on N_{H} and the source’s effective temperature. Sources with low temperatures are more difficult to detect if significant N_{H} -absorption takes place.

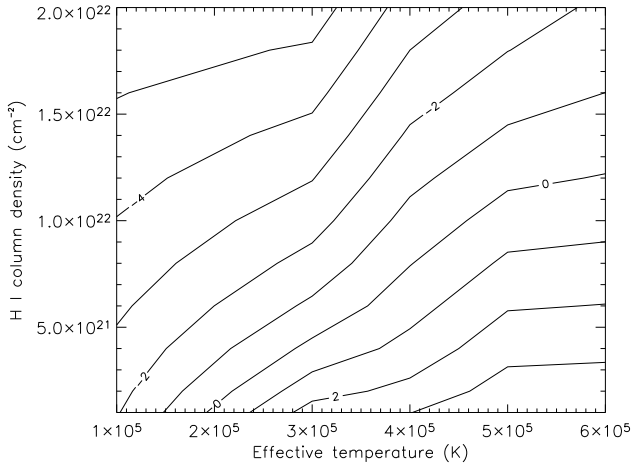


FIG. 2.— Contour plot of the \log_{10} Swift counts predicted with a 1-ksec observation from a SSS as a function of temperature (Cloudy model) and interstellar extinction (N_{H}) for a source at a distance of 1 kpc.

Without long (> 10 ksec) exposures, $N_{\text{H}} \sim 10^{22} \text{ cm}^{-2}$ is the highest number that allows a detection of SSS emission at 1 kpc distance with *Swift*. Since most novae are further away than 1 kpc, the situation is even worse.

2.3. Targets

Although primarily a mission to study the temporal evolution of γ -ray bursts (GRB), *Swift* also provides Targets of Opportunity (ToO) observations for non-GRB events. Through ToO observations we have obtained X-ray observations of 9 recent ($< 1-2$ years since outburst) and 3 older (> 3 years) CNe. We consider all observations, although those of V1188 Sco on 21 May, 2006 and of V574 Pup taken on 26 July, 2005 were extremely short with hardly any signal. Table 1 provides a list of important physical parameters associated with these novae including the maximum visual magnitudes, the date of discovery, the time to decline 2 magnitudes from maximum (t_2), the early measured expansion velocities, $E(B - V)$ reddening values, H I column densities, and distances. In the appendix A.1 we summarize background information for each nova in our sample.

3. ANALYSIS OF THE *Swift* XRT DATA

Currently the *Swift* archive contains 27 observations of 12 novae obtained with the X-ray Telescope (XRT) instrument (see Sect. 2.1). We analyzed the data using the *Swift* reduction packages in HEASoft version 6.06⁸ and the latest calibration data (version 20060427). We started with the photon event files (level 2) that are available in the public *Swift* archive and carried out three statistical tests to determine if the sources were detected. We then calculated count rates or upper limits in cases where no detections can be claimed. The first criterion is the formal detection likelihood from comparison of the number of counts measured in the source extraction region (circular with 10 pixels radius around expected sky position) with the background extraction region (annulus around source extraction region with inner radius 10 pixels and outer radius of 100 pixels). We next determined if there was a concentration of counts near the

center of the source extraction region. Finally, we compared the spectral distributions of photons in the source and background extraction regions, but this is only a soft criterion, as similar spectral distributions do not rule out the presence of a source. We present our statistical methods in more detail in the appendix Sect. A.2 to justify our tests.

In Table 2 we provide all the *Swift* observational data including observation date, time since visual maximum, exposure time, number of counts in the source and background extraction regions, and either the net source count rate per detect cell with 1σ uncertainty, or the upper limit.

3.1. Non-detections, failure of all criteria

Only upper limits could be established for the observations of V476 Sct, V1188 Sco, LMC 2005, and V1494 Aql.

In Fig. 3 we show the photon plot centered around the expected source position of V476 Sct and LMC 2005. The extraction regions for source and background, as defined in Sects. 3 and A.2 are marked with dark and light gray colors, respectively, and the counts within the source extraction region are plotted with small black bullets. In the upper right corner we list: the date of observation, source extraction region, the number of counts in the respective extraction regions, and the exposure times. In the upper left corner we display the source net count rate (or the 95.5-% upper limit if no significant excess count rate is found) as well as the detection likelihood, the number of net source- and background counts S and B , respectively, as defined in Eq. A1. For V1188 Sco, all criteria fail for all observations, and the source is clearly not detected. A similar case is encountered for all three observations of LMC 2005, where we show the last observation in the right panel of Fig. 3. Further, we found no significant detections in all three observations of V1494 Aql. We found only a marginal detection in the *Chandra* observation of V1494 Aql five years prior to the *Swift* observations (see Sect. 3.4). We used the proposal planning tool PIMMS in order to convert the *Chandra* count rate into an expected *Swift* XRT count rate. With various model assumptions PIMMS predicts more than 0.04 XRT counts per second, while we measured less than 0.0014 counts per second in each observation (Table 2). This implies that the source has faded by at least a factor 30 within five years.

3.2. Weak sources < 0.01 cps

V1663 Aql was the first nova observed by *Swift*. Unfortunately, the first planned observation was truncated by a GRB after only 1.25 ksec. Nevertheless, we find a clear detection and a strong concentration of counts towards the center (Table 2). The source spectrum is similar to the background spectrum, but that does not rule out a detection (see Fig. 4). The spectrum is extremely weak and no conclusion can be drawn. A second observation seven months later was longer but yielded only an upper limit which implies a fading of the source. Neither of our other two criteria supported a detection.

For V5116 Sgr we only found a marginal (formal 93-percent) detection with a concentration of photons towards the center. The spectrum is too weak to apply our source-background comparison criterion (see Fig. 5).

⁸ <http://swift.gsfc.nasa.gov/docs/software/lheasoft/>

TABLE 1
BASIC NOVA PARAMETERS

Object	V_{max} (mag)	Date ^a	t_2 ^b (days)	v_{exp} ^c (km sec ⁻¹)	E(B-V) (mag)	N_H ^d (cm ⁻²)	Dis. (kpc)	Refs. ^e
V574 Pup	8	11/26/2004	13	650H,860P	1.27	6.5e21	3.20	1,2,3
V382 Nor	9	03/19/2005	13	1100P	0.6-1.1	1.8e22	13.80	3,3,3
V1663 Aql	10.5	06/10/2005	16	700P	~2	1.8e22	5.5±1	4,5,4
V5116 Sgr	<8	07/04/2005	20	1300P	0.24±0.08	1.6e21	11.30	3,3,3
V1188 Sco	8.9	07/26/2005	12	1730H,4000Z	~1?	5.0e21	7.5	3,3,3
V1047 Cen	8.83	09/04/2005	?	850H	3.3?	1.6e22	?	-,3,-
V476 Sct	10.9	09/30/2005	15	1200H	1.9±0.1	1.1e22	4±1	6,6,6
V477 Sct	10.4	11/10/2005	3	2700H,6000Z	>1.3	4.8e21	11	7,7,7
LMC2005	12.6	11/27/2005	?	-	0.15	6.3e20	50	3,3,3
V723 Cas	7.1	12/17/1995	slow	700H	~0.5	2.4e21	4	-,8,9
V1494 Aql	4	12/03/1999	6.6±0.5	1300H,1850P	0.6±0.1	4.2e21	1.6±0.2	10,-,11
V4743 Sgr	5	09/20/2002	9	2400H	low?	1.4e21	6.3	3,-,12

^a Date of visual maximum (mm/dd/yyyy).

^b Time to decline 2 magnitudes from maximum.

^c Expansion velocity. Taken from early IAU circulars. Trailing letters indicate how the velocity was measured: H = Full-Width at Half-Maximum, P = P Cygni absorption, Z = Full-Width at Zero-Intensity.

^d The HI column densities were obtained from the Heasarc NH tool. They are the line-of-sight column densities through the entire Galaxy toward the coordinates of each object.

^e References for t_2 , E(B-V), and Distance:

1 = Siviero et al. (2005); 2 = Rudy, private communication; 3 = t_2 : from AAVSO light curve and IAU circulars. E(B-V): using van den Bergh & Younger (1987) and the (B-V) color evolution or assuming E(B-V) $\sim N_H/4.8 \times 10^{21}$ cm⁻². Distance: using the M_V vs t_2 relationship of Della Valle & Livio (1995); 4 = Lane et al. (2006); 5 = Puetter et al. (2005); 6 = Munari et al. (2006b), Perry et al. (2005); 7 = Munari et al. (2006a); 8 = Munari et al. (1996); 9 = (Iijima et al. 1998); 10 = Kiss & Thomson (2000); 11 = Iijima & Esenoglu (2003); 12 = Lyke et al. (2002).

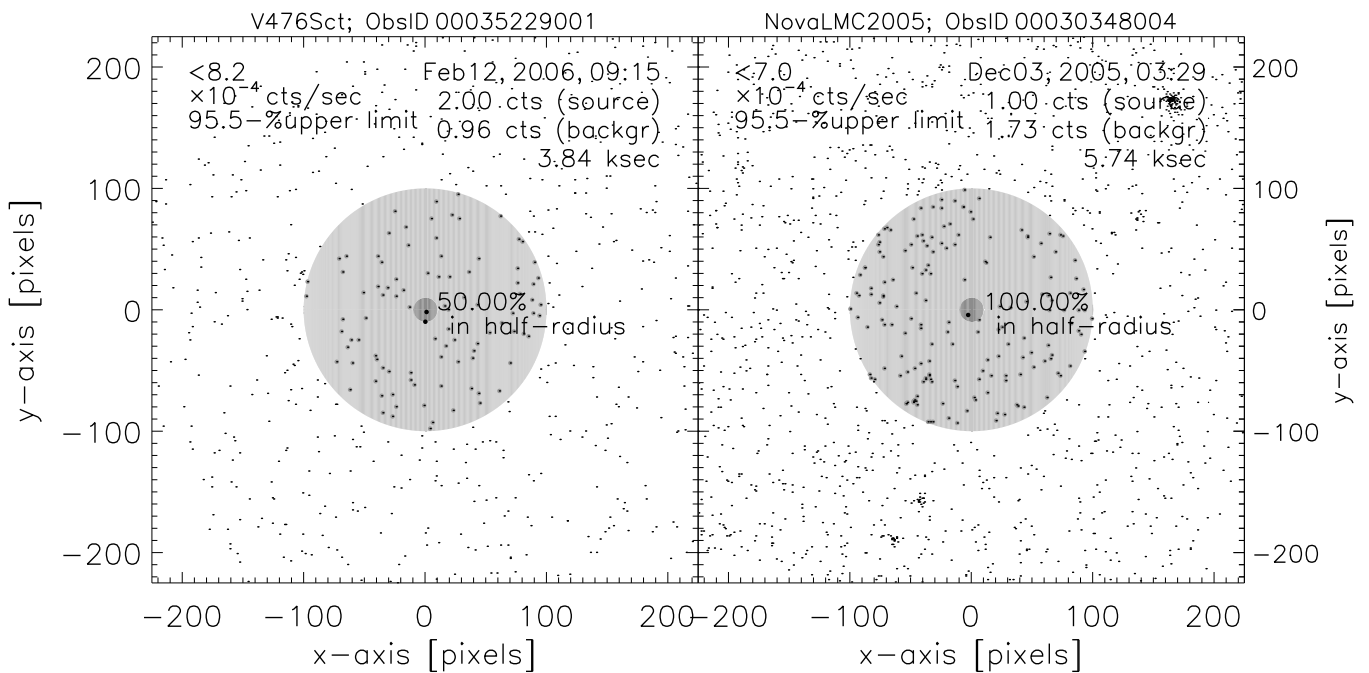


FIG. 3.— V476 Sct (left) and LMC2005 (right) were not detected. We show the recorded photon positions and mark the source extraction region with dark shading and the background extraction region (annulus with inner radius 10 pixels and outer radius 100 pixels) with light shading. The pixel- and sky coordinates are given in the bottom. The upper limits are given in the upper left. Observation date, extraction radius, number of source- and background counts per detect cell, and exposure time are given in the upper right. The percentage of source counts that reside within 25 percent area (radius 5 pixels) is given to the right of each source extraction region to give an impression of the concentration towards the center within the source extraction region.

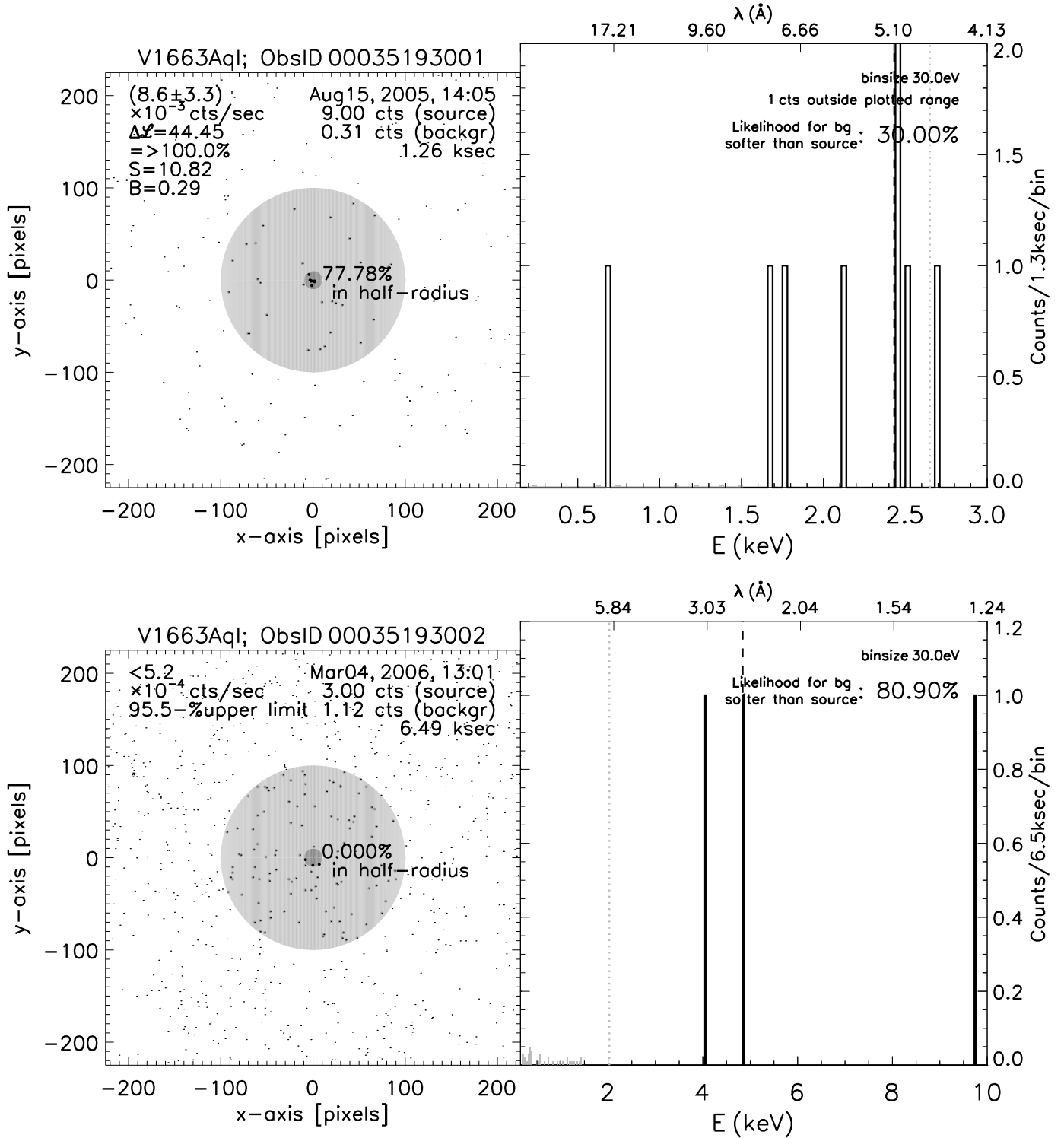


FIG. 4.— Two *Swift* observations of V1663 Aql. The left panels (image) are the same as described in Fig. 3. The right panels provide the spectral information of the source (black) and background (downscaled to the area of the source extraction region; light shadings). The likelihood for the background spectrum being softer than the source spectrum is estimated by drawing 1000 random sample spectra with the number of source counts (in the upper panel 9) out of the background ($0.31 \times 99 = 31$ counts) and counted the number of cases where the median energy of each sample spectrum was lower than that of the source spectrum. Much different values than 50 percent are a soft criterion for a source detection. In the upper panel we find a clear detection and give the count rate with $1\text{-}\sigma$ uncertainty, $\Delta\mathcal{L}$ according to Eq. A6, and the number of net counts for source and background S and B (per detect cell) according to Eq. A1.

TABLE 2
MEASURED COUNT RATES IN OUR SAMPLE

Start Date	Δt^a (d)	Exp. (ks)	Src. (cts) ^b	Bg. (cts) ^b	Rate ^{b,d} (cts/ks)	$R_{1/2}^c$ (%)
V574 Pup						
05/20/2005	175	1.0	10	0.4	12.0 ± 4.0	60
05/25/2005	180	1.9	22	0.4	14.0 ± 3.0	77
05/26/2005		0.01	0	0	0	0
07/29/2005	245	1.1	15	0.3	16.0 ± 4.0	67
07/30/2005	246	7.1	51	2.1	8.5 ± 1.3	73
08/06/2005	253	7.8	57	2.0	8.7 ± 1.2	67
08/09/2005	256	2.2	22	0.6	12.0 ± 3.0	64
08/10/2005	257	2.8	18	0.8	7.8 ± 2.0	67
08/11/2005	258	1.8	11	0.5	7.3 ± 2.5	56
08/17/2005	264	4.7	34	1.2	8.6 ± 1.6	79
V382 Nor						
01/26/2006	313	6.1	72	4.0	14.0 ± 2.0	75
V1663 Aql						
08/15/2005	66	1.3	9	0.3	8.6 ± 3.3	78
03/04/2006	267	6.5	3	1.1	$< 0.5^d$	0
V5116 Sgr						
08/29/2005	56	3.1	5	2.0	1.2 ± 1.0	80
V1188 Sco						
05/21/2006	98	0.2	1	0.1	$< 7^d$	0
06/17/2006	124	5.0	3	2.3	$< 9.1^d$	33
V1047 Cen						
09/11/2005	66	3.9	19	1.3	5.6 ± 1.5	53
01/23/2006	141	5.3	53	3.1	11.0 ± 2.0	72
V476 Sct						
02/12/2006	135	3.8	2	1.0	$< 8.2^d$	50
V477 Sct						
03/07/2006	117	6.2	15	1.8	2.7 ± 0.8	87
03/15/2006	125	4.7	8	1.3	1.8 ± 0.8	50
LMC 2005						
12/02/2005	5	0.1	0	0.1	$< 1.0^d$	0
12/01/2005	4	4.1	1	1.3	$< 8.6^d$	100
12/02/2005	5	3.9	2	1.2	$< 8.7^d$	100
12/03/2005	6	5.7	1	1.7	$< 7.0^d$	50
V723 Cas						
01/31/2006	3698	6.9	147	1.7	26.0 ± 2.0	69
V1494 Aql						
03/10/2006	2289	1.4	0	0.3	$< 1.4^d$	0
03/13/2006	2292	1.2	0	0.2	$< 1.4^d$	0
05/19/2006	2359	2.5	1	0.5	$< 1.0^d$	100
V4743 Sgr						
03/08/2006	1265	5.8	267	2.3	27.0 ± 2.0	70

^a Interval between visual maximum and the XRT observation in days

^b per detect cell (10 pixels radius); count rates with 1σ uncertainties

^c fraction of counts within 5 pixels (%)

^d 95.5-% upper limit

Two observations of V477 Sct were carried out 8 days apart and resulted in two detections with a likelihood > 99 percent (see Fig. 6). The first observation suggests a weak source with a clear concentration towards the center and a much softer spectrum than that of the instrumental background. The second observation reveals a lower count rate, lower detection likelihood, and a less clear concentration of photons towards the center. While this implies variability or that the source has faded over the eight day interval, within the $1\text{-}\sigma$ errors, the count rate is consistent with that of the first observation. Neither spectrum allows quantitative analysis.

3.3. Strong sources > 0.01 cps

V574 Pup, V382 Nor, V1047 Cen, V723 Cas, and V4743 Sgr were detected by *Swift* (see Figs. 7–11).

The spectrum of V382 Nor is hard whereas the background is softer. There appears to be some excess emission at wavelengths of prominent emission lines (e.g., 0.92 keV, Ne IX; 1.02 keV, Ne X; and 0.83 keV, Fe XVII) but a firm identification of these lines is not possible with the existing data. There is also emission at energies with no well-known emission lines, particularly at high energies. The observed spectrum is too faint to derive any quantitative conclusions.

We obtained very clear detections of V1047 Cen. In the first observation of November 2005 the photons are clearly concentrated towards the center, and the energy distribution is very different from the soft background. Two months later the detection is even stronger and the spatial as well as spectral distributions clearly support a detection. The count rate doubled from 5.6 cts ksec⁻¹ on 9 November, 2005 to 11 cts ksec⁻¹ on 23 January, 2006. The spectrum appears hard, but there are too few counts to derive any spectral properties.

The remaining novae were sufficiently bright to obtain spectral confirmation that they were detected during the SSS phase. More detailed analysis of these spectra, including additional *Swift* observations and supporting optical and near-IR spectra, is left for future papers. Here we only provide a brief analysis of the current *Swift* data sets.

V574 Pup was first observed in late May 2005. It was then observed multiple times from the end of July to mid August 2005 as it was perfectly positioned to cool the XRT detectors between GRB observations. In all nine observations, it was clearly detected with a high degree of significance (see Table 2). V574 Pup had an average of $7 - 14$ cts ksec⁻¹ in each observation. The individual observations were too short for analysis, so we combined them, yielding a higher signal-to-noise ratio. We grouped the spectra by summing the number of counts and the number of background counts in each spectral bin. We calculated exposure time-weighted effective areas from the individual extracted effective areas.

However, during the 50 days between the May 26 and July 29, significant evolution probably occurred which we would miss by combining all spectra together. In order to search for any evolution, we grouped the first two observations from May 2005 and the remaining observations from July and August 2005. These are shown in Fig. 12. The summed spectra of the two early observations shows a uniform distribution with energy and may be an underexposed emission line spectrum. Unfortunately, we don't

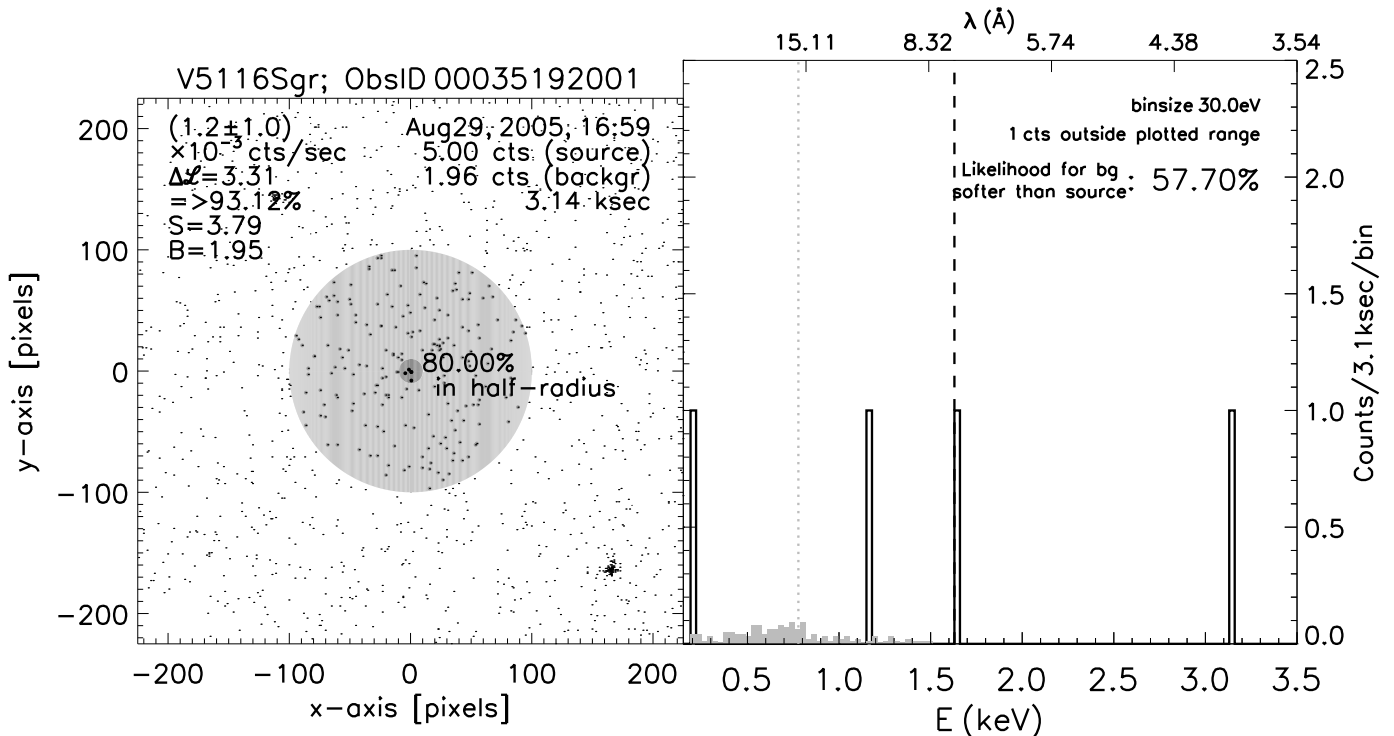


FIG. 5.— Same as Fig. 4 but for V5116 Sgr.

have any more data from this time period to increase the signal-to-noise ratio. The later observations sum up to what appears to be a continuous spectrum ranging from 0.3–0.5 keV (25 Å to 45 Å). This spectrum resembles that of a SSS. We carried out a blackbody fit using the most recent XRT response matrices (version 8) and assuming an emitting radius of 7000 km. We found a satisfactory fit (Fig. 13) with the parameters $T_{\text{eff}} = (293 \pm 10) \times 10^3$ K (25.2 ± 1 eV) and $N_{\text{H}} = (2.5 \pm 0.6) \times 10^{21}$ cm $^{-2}$ (1- σ uncertainty ranges). We fixed the radius because no unique solution could be found with a variable radius. The uncertainties include variations of the radius between 7000 and 9000 km.

The XRT spectrum of V4743 Sgr is faint, and no spectral features can be identified. We also found no features in the RGS observation taken in September 2004 (see below). While the XRT count rates of V4743 Sgr and V723 Cas are similar, the spectra are different (Fig. 11). V723 Cas shows a clear peak occurring at 0.4 keV (31 Å). Ness et al. (2006b) reported that the spectrum resembled a SSS, and they were able to fit a blackbody model. We repeated these fits using the updated XRT response matrices (version 8) and show the best-fit model in Fig. 14. We fixed the radius at 7000 km but included variations up to 9000 km in the calculation of the 1- σ uncertainty ranges. We find $T_{\text{eff}} = (371 \pm 15) \times 10^3$ K (32 ± 2 eV) and $N_{\text{H}} = (3.3 \pm 0.4) \times 10^{21}$ cm $^{-2}$. V723 Cas is now, after 11 years, the oldest Galactic nova that is still active. Such a long duration of the SSS phase is unusual for a Classical Nova, and there is a possibility that the nova has transitioned into a SSS such as Cal 83. Our observations of this interesting source are continuing.

3.4. Supplemental observations

In addition to the *Swift* observations, we extracted unpublished X-ray observations from the *Chandra* and *XMM-Newton* archives.

A series of *Chandra* observations of V1494 Aql were carried out and we extracted the last observation (LETGS, ObsID 2681) taken 727 days after outburst (2001, Nov. 28). The source was only detected in the zeroth order on the HRC-S detector, but no dispersed spectrum could be extracted. We found 56 counts on a background of 10, corresponding to an HRC count rate of 0.02 ± 0.003 cts sec $^{-1}$ and a 14- σ detection. Unfortunately, the HRC detector does not provide the energy resolution to construct a spectrum, and no spectrum can be constructed from the dispersed photons as the background is too high.

We further analyzed *XMM-Newton* observations of LMC 2005 taken 243 days after outburst (ObsID 0311591201, 2006, July 18) and of V4743 Sgr 1470 days after outburst (ObsID 0204690101, 2004, Sept. 30). LMC 2005 was again not detected.

From MOS1 we extracted 0.11 ± 0.002 cts sec $^{-1}$ for V4743 Sgr. The source was also detected in the RGS with a count rate of 0.01 ± 0.0005 cts sec $^{-1}$. Grating spectra allow the calculation of a flux without the need of a model, and we measured a flux of 3×10^{-13} erg cm $^{-2}$ sec $^{-1}$ from the RGS1 and RGS2⁹. Fig. 15 shows a comparison of these last *XMM-Newton* spectra with the recent *Swift* observation.

4. DISCUSSION

The sample of X-ray observations of novae presented in this paper demonstrates that *Swift* significantly increased the number of Galactic novae observed in X-

⁹ 0.35–1.8 keV; corrected for the chip gaps

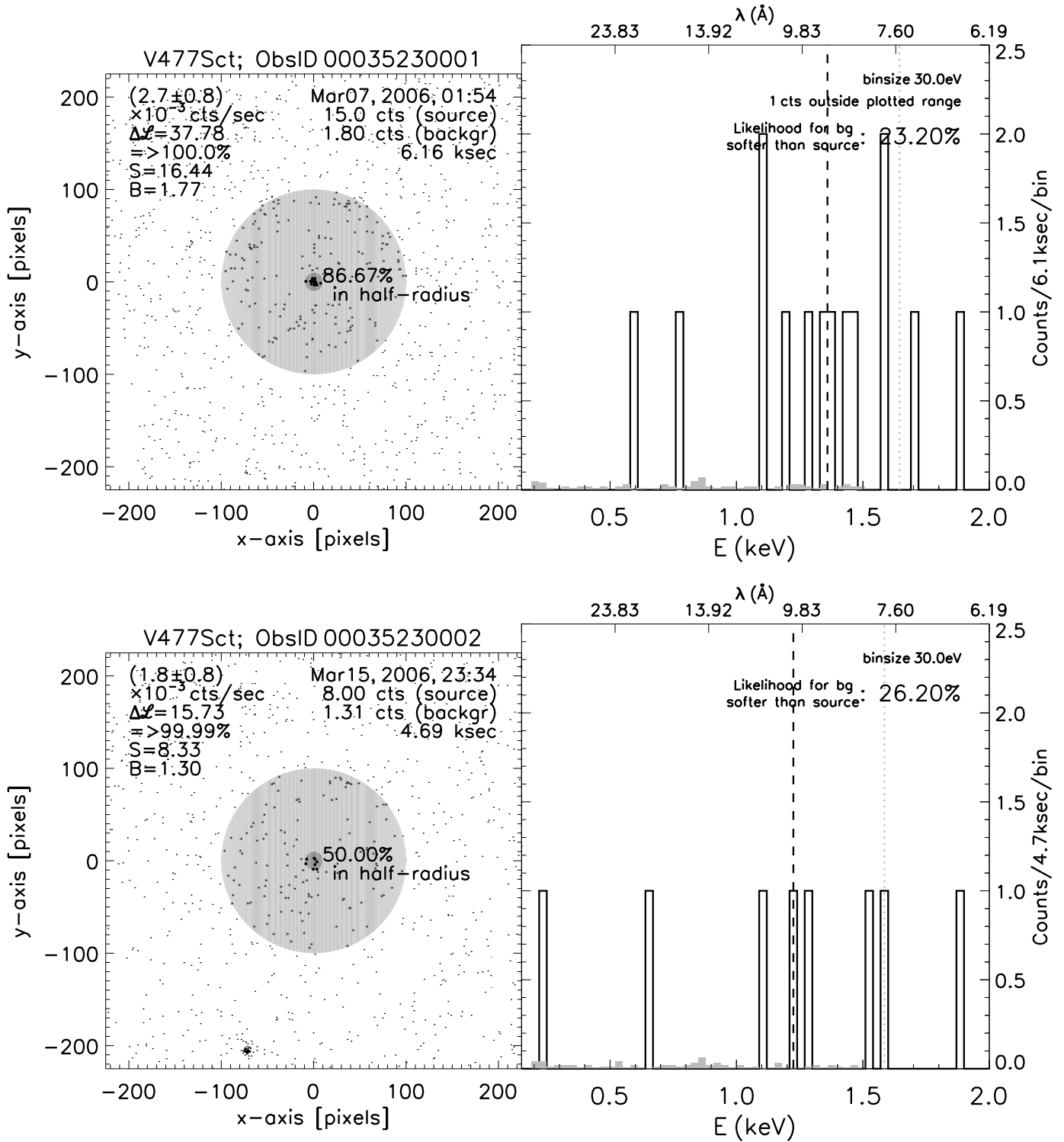


FIG. 6.— Same as Fig. 4 but for the two observations V477 Sct.

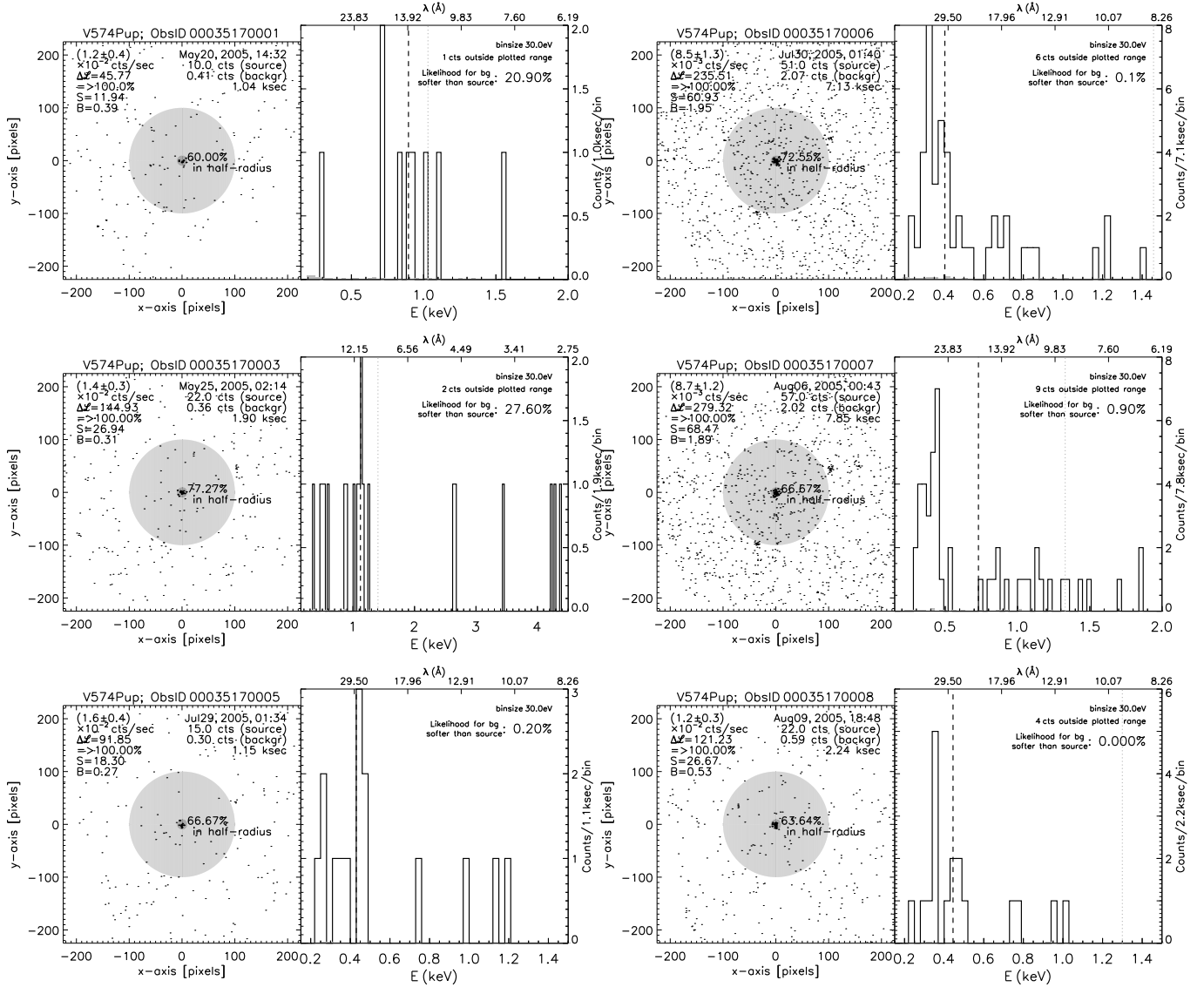


FIG. 7.— Same as Fig. 4 but for six usable observations of V574 Pup.

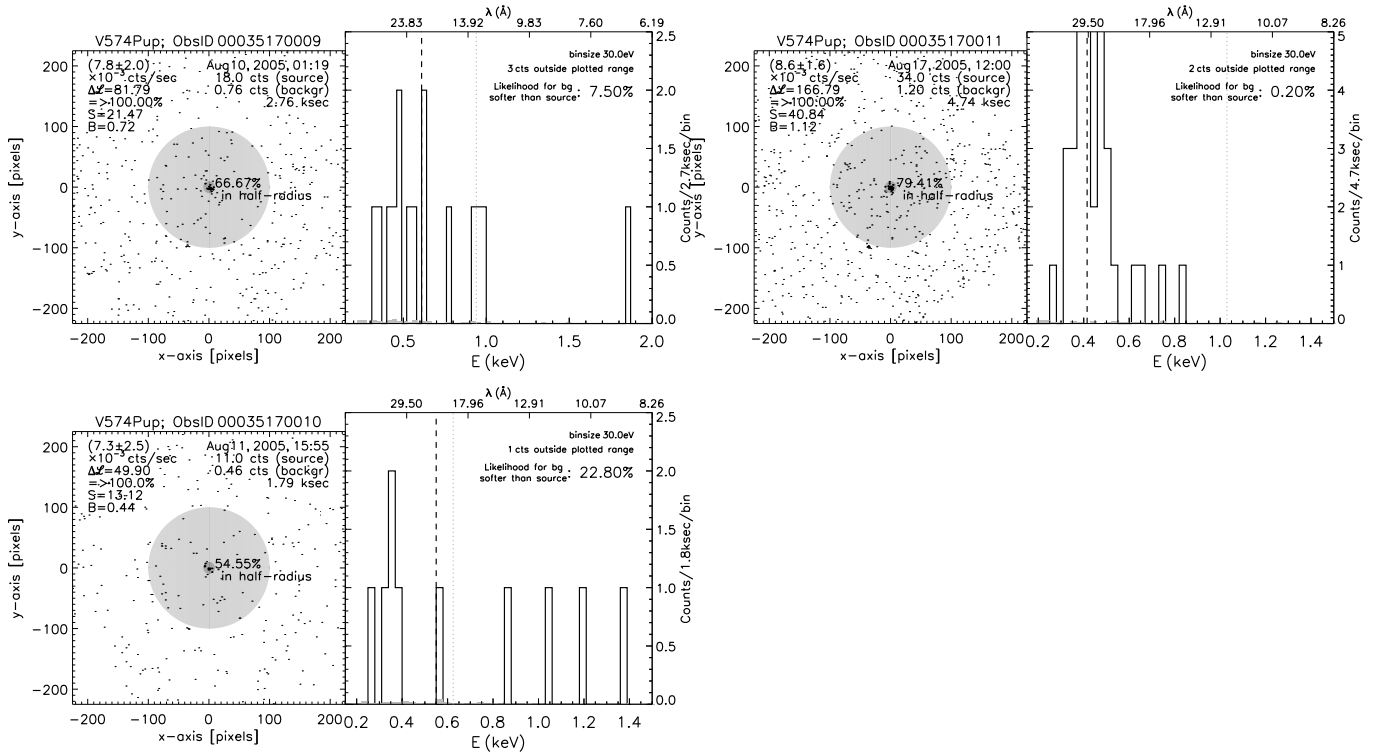


FIG. 8.— Continuation of Fig. 7.

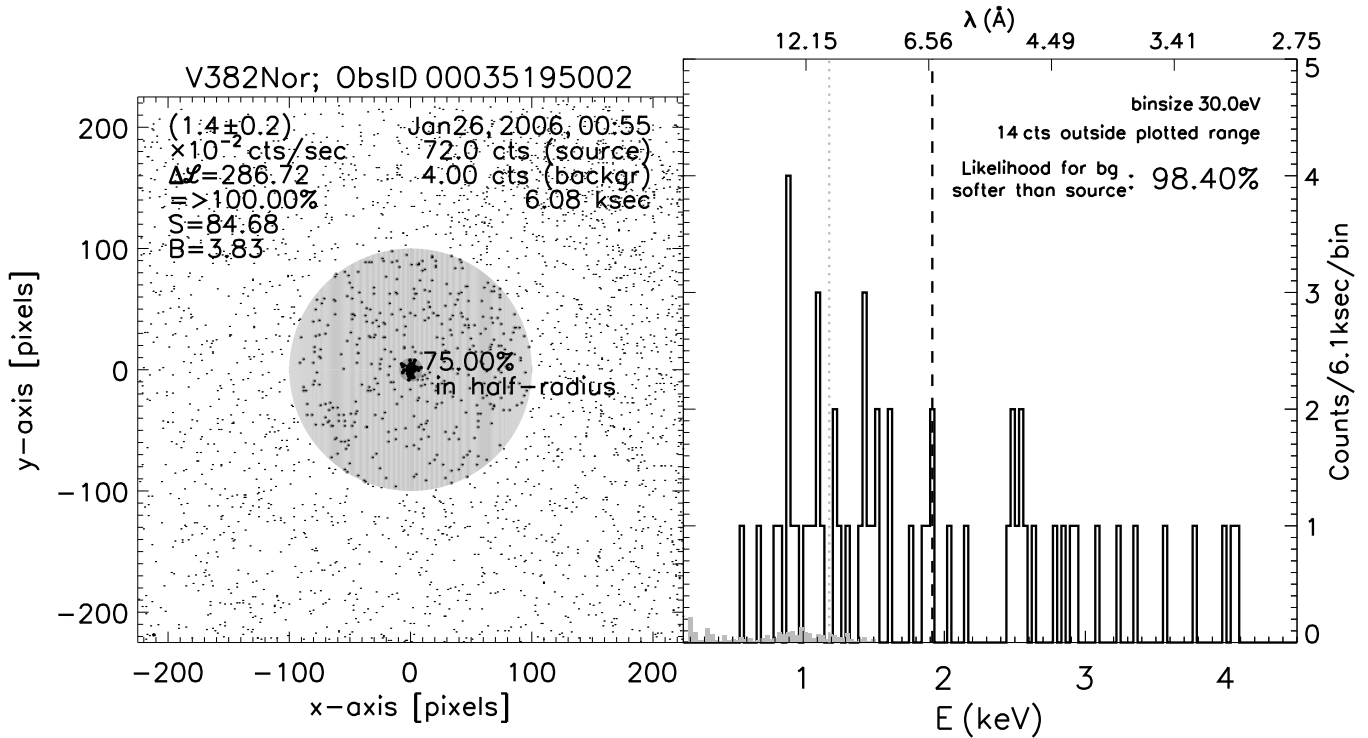


FIG. 9.— Same as Fig. 4 but for V382 Nor. The spectrum appears to be an emission line spectrum, but we note that it is oversampled and the lines cannot be as clearly identified.

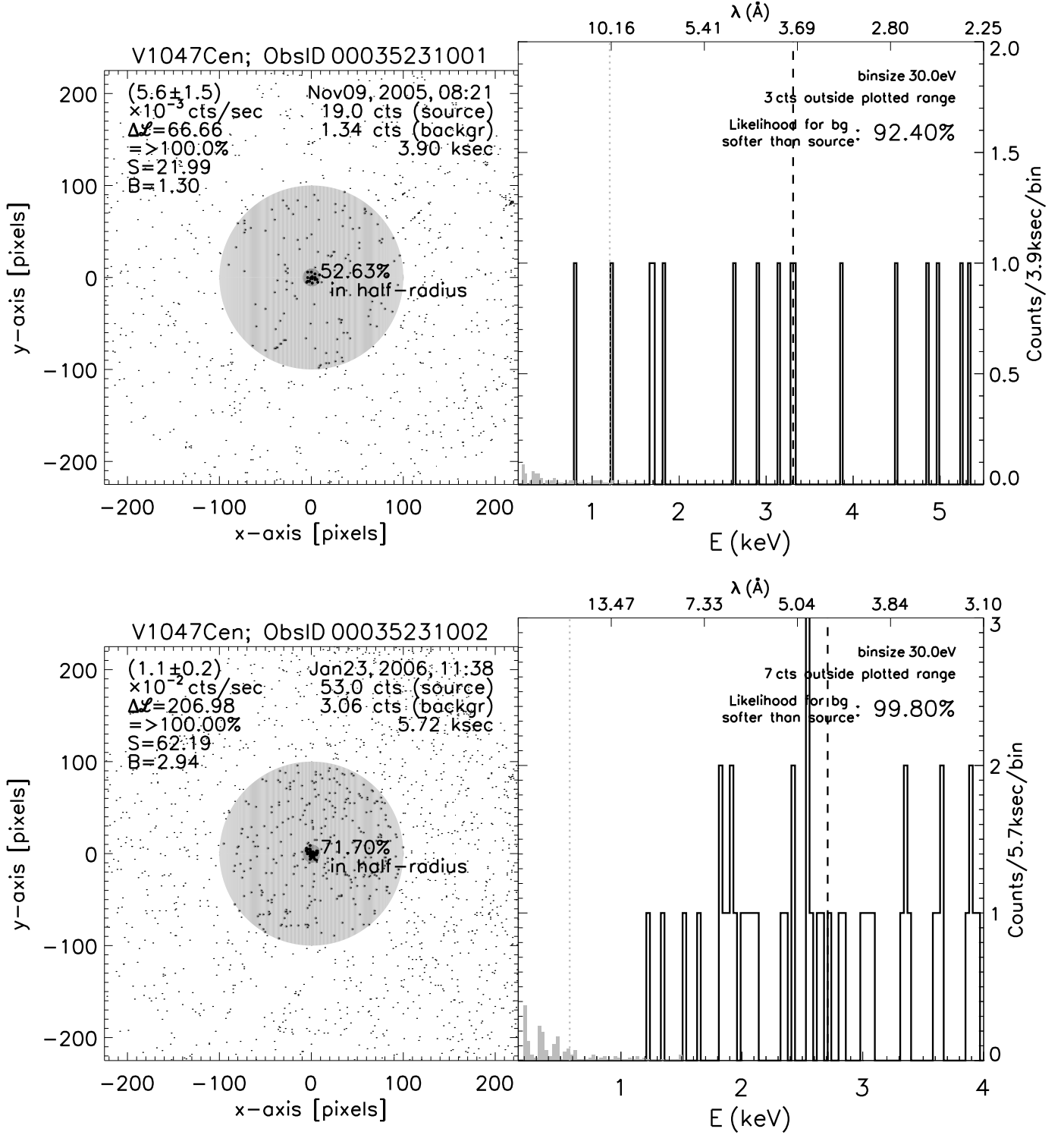


FIG. 10.— Same as Fig. 4 but for the two observations of V1047Cen.

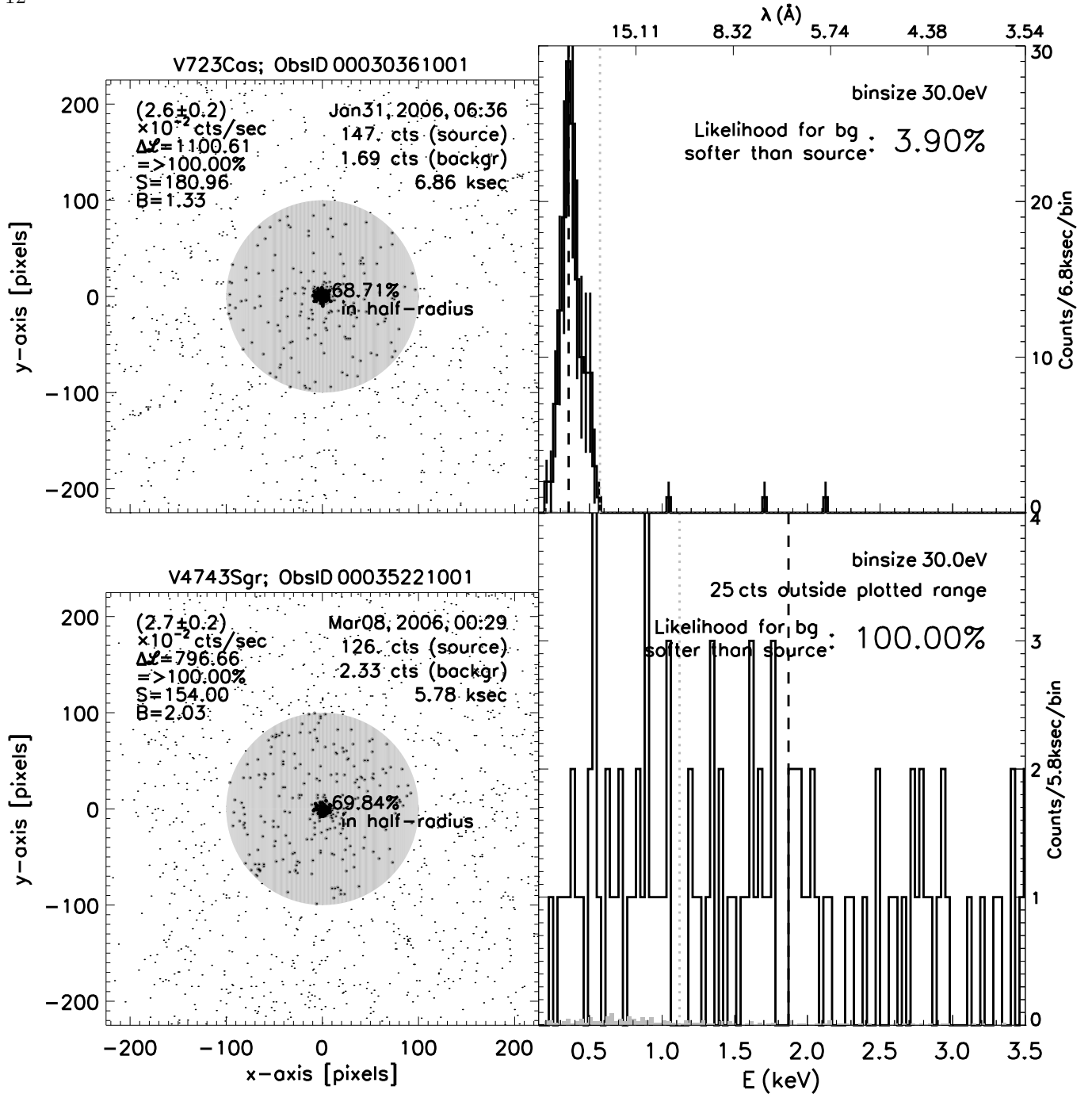


FIG. 11.— Same as Fig. 4 but for V723 Cass (top) and V4743 Sgr (bottom). While the count rates are similar, the spectra are very different.

rays. We provide a large sample taken with the same instrument, which reduces problems from cross calibration. Also, *Swift* is capable of carrying out monitoring observations with relatively little effort, the exception being classical novae with large column densities. In Sect. 2.2 we demonstrated that one can not obtain enough counts in a typical ToO exposure (3–5 ks) when the column density exceeds $N_H > 10^{22} \text{ cm}^{-2}$ to observe an SSS phase. In this survey the estimated column densities of four novae, V382 Nor, V1047 Cen, V1663 Aql, and

V476 Sct, exceeded this value and only very hard spectra or non-detections were recorded. For Galactic novae with low column densities *Swift* is an excellent instrument for following all the stages of evolution in X-rays (e.g., the recurrent nova RS Oph Osborne et al. 2006).

Shortly after the outburst, X-ray emission from the WD is not expected to be observed. X-ray detections during this phase thus originate from other processes, e.g., shocks within the expanding shell or a shock set off by a collision between the expanding shell and the atmo-

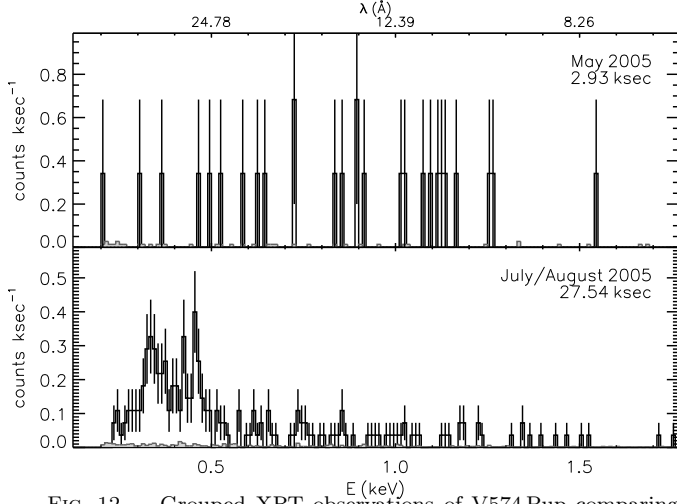


FIG. 12.— Grouped XRT observations of V574 Pup comparing the May 2005 (top panel) and the July through August data sets (bottom panel). The comparison shows that V574 Pup has evolved from a hard early spectrum (top panel) into a SSS spectrum (bottom). The count rate is higher in the top panel, which may be due either to the higher sensitivity of the detector at higher energies or the higher amounts of absorption at soft energies.

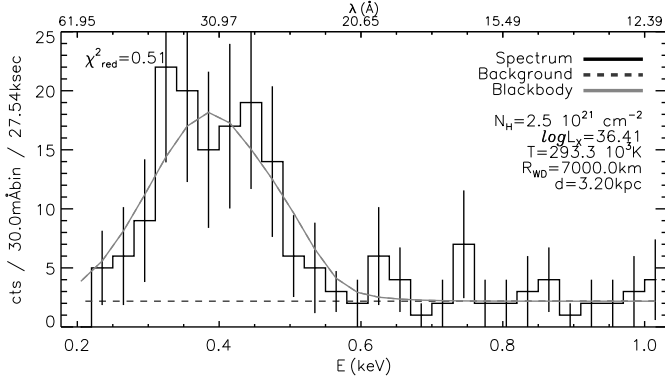


FIG. 13.— Grouped and rebinned XRT spectrum of V574 Pup covering from July 2005 to August 2005 (shown in the bottom panel of Fig. 12). The histogram (plus error bars) gives the observed spectrum and smooth line shows the best-fit blackbody model overplotted (parameters given in legend).

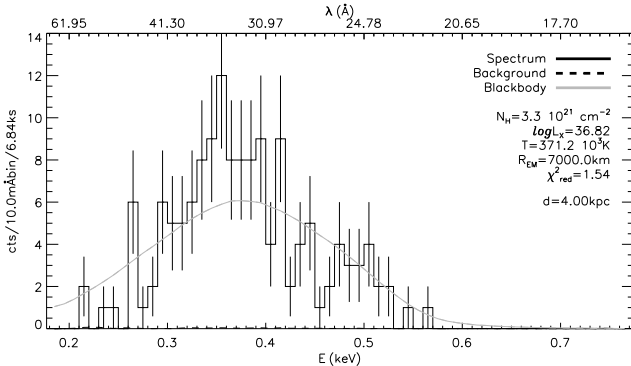


FIG. 14.— Blackbody fit to the XRT spectrum of V723 Cas. The background lies on top of the horizontal axis.

sphere of the companion (as in RS Oph, e.g., Bode et al. 2006). Few observations during this phase have been carried out (e.g. Mukai & Ishida 2001) and they only provide information on dynamics within the ejecta. With the flexibility of *Swift* a better assessment of pre-SSS X-ray emission can be achieved.

The SSS phase is the brightest phase of X-ray emission

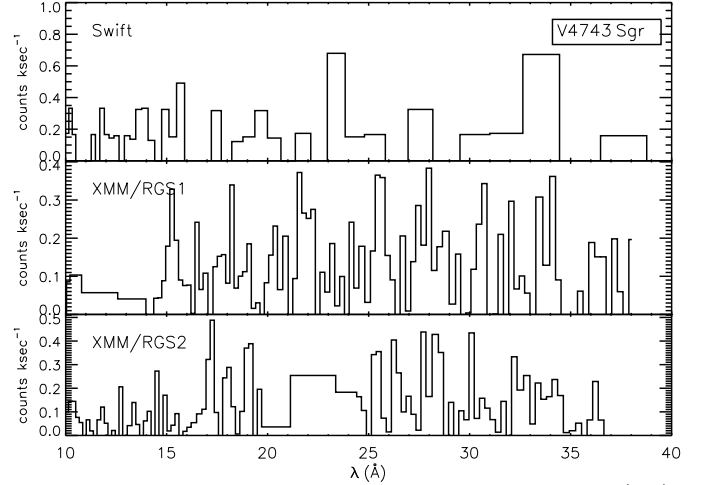


FIG. 15.— Comparison of the XRT spectrum of V4743 Sgr (top) with *XMM-Newton* RGS1 and RGS2 spectra from September 2004. All are consistent with a fading nebular spectrum, but the signal to noise and the resolution are insufficient to characterize the spectrum as hard continuum or an emission line spectrum.

(at constant bolometric luminosity), making it the best time to observe a nova. We found two clear detections of novae in this phase. With these two new SSS spectra, the number of Galactic novae clearly observed in this state is seven (Orio et al. 2001b; Drake et al. 2003; Ness et al. 2003, and reference therein). For V574 Pup we were even able to identify the transition from an early emission line spectrum to a bright SSS spectrum within two months. V574 Pup entered its SSS phase within 250 days after outburst. This is consistent with the evolution of V1974 Cyg, V1494 Aql, and V4743 Sgr (see Fig. 16). The detection of a SSS in V723 Cas suggests that nuclear burning is still going on more than 11 years after outburst. It is not known how much longer it will remain a SSS. More detailed discussions on V723 Cas will be presented by Ness et al. (in prep).

We detected V4743 Sgr two years after *XMM-Newton* had already measured a very low level of X-ray emission (see Sect. 3.4). This shows that the post-turn-off evolution can last a few years. V1494 Aql was not detected, but five years prior to our observation it had been found to have marginal emission and no SSS spectrum.

In order to compare the evolution of the novae detected in our sample we plot their distance-scaled X-ray brightnesses as a function of individual time after outburst in Fig. 16. In the bottom panel we show the X-ray light curves (in the same time units) of five more Galactic novae, but observed by different missions. The brightness is given as unabsorbed luminosity as extracted from direct measurements of fluxes (Greiner et al. 2003b; Orio et al. 2001a; Balman et al. 1998; Ness et al. 2003; Petz et al. 2005). As a general rule, any X-ray detection of novae earlier than 100 days after outburst arises from the hard, shock-generated phase that can either be emission lines or possibly bremsstrahlung emission (Orio et al. 2001a; Mukai & Ishida 2001). Likewise, any X-ray detections more than 1000 days after outburst come from the nebular phase, with the three exceptions of GQ Mus, LMC 1995, and now V723 Cas. These general rules also hold for novae in M31 (see figure 3 in Pietsch et al. 2005).

Finally, we can use the parameters derived from the

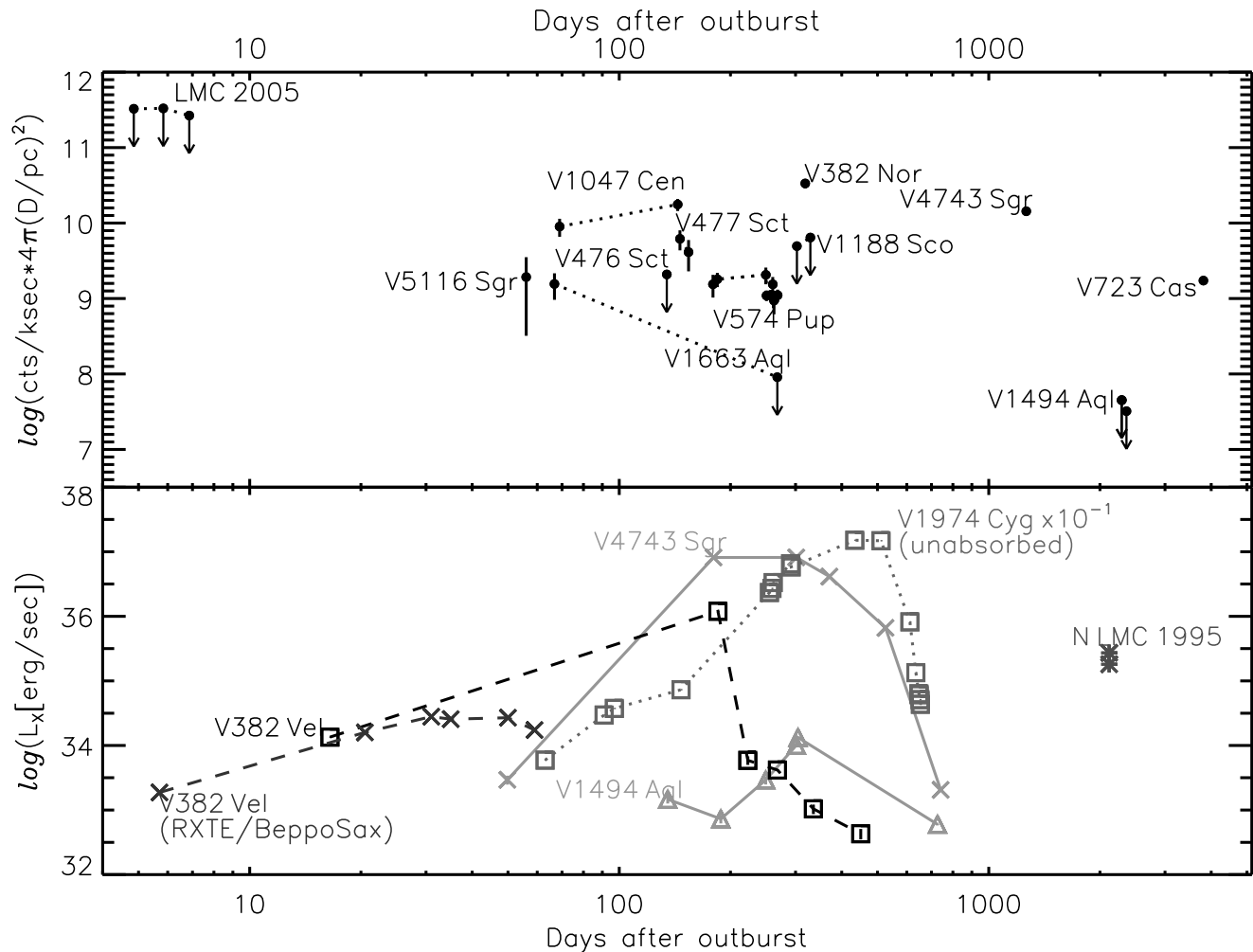


FIG. 16.— **Top:** XRT count rates of all sources in our sample, plotted against the day of observation after their outbursts. The count rates are corrected for distance squared which is uncertain. Multiple observations of the same targets are connected with dotted lines. **Bottom:** Observations from various other missions. The observed X-ray luminosities (not corrected for absorption, except for V1974 Cyg, which is instead rescaled) of recent well-observed novae with SSS phases. Similar plots have been created by Pietsch et al. (2005); Pietsch et al. (2006).

model fits to the SSS spectra of V574 Pup and V723 Cas to check the *Swift* counts that we predicted from our attenuated Cloudy model of an “average” classical nova ejection in Fig. 2 (Sect. 2.2). From our blackbody fits we obtained effective temperatures of $\sim 3 \times 10^5$ K (25 eV) for both novae, while the derived column densities were 2.7 and $1.7 \times 10^{21} \text{ cm}^{-2}$ for V574 Pup and V723 Cas, respectively. With these parameters we find from the grid of Cloudy models (Fig. 2) the predicted counts in a 1-ksec observation at a distance of 1 kpc of ~ 10 for V574 Pup and ~ 100 for V723 Cas. Scaling these predicted counts by the distances in Table 1 and the exposure times in Table 2 ($t_{exp}(\text{ksec})/D(\text{kpc})^2$) gives 75 counts for V723 Cas and 7 counts for the 30 July, 2005 observation of V574 Pup. These values are consistent with the detections given the uncertainties in the distances and the use of a generalized nova model (*e.g.* a luminosity of $10^{38} \text{ erg s}^{-1}$, an ejected mass $\sim 10^{-4} M_{\odot}$,

Schwarz et al. 2007). For “normal” classical novae, calculations like those done for Fig. 2 can be used as a tool to plan X-ray observations by providing first-order estimates of expected X-ray brightness levels during the SSS phase.

We acknowledge the use of public data from the *Swift* data archive. We acknowledge with thanks the variable star observations from the AAVSO International Database contributed by observers worldwide and used in this research. J.-U. N. gratefully acknowledges support provided by NASA through Chandra Postdoctoral Fellowship grant PF5-60039 awarded by the Chandra X-ray Center, which is operated by the Smithsonian Astrophysical Observatory for NASA under contract NAS8-03060. S. Starrfield received partial support from NSF and NASA grants to ASU. JPO acknowledges support from PPARC

Facilities: Swift (XRT), XMM, CXO

REFERENCES

- Avni, Y. 1976, ApJ, 210, 642
 Balman, S., Krautter, J., & Ögelman, H. 1998, ApJ, 499, 395
 Bode, M. F., O’Brien, T. J., Osborne, J. P., Page, K. L., Senziani, F., Skinner, G. K., Starrfield, S., Ness, J.-U., Drake, J. J., & Schwarz, G. 2006, ApJL, accepted

- Burrows, D. N., Hill, J. E., Nousek, J. A., Kennea, J. A., Wells, A., Osborne, J. P., Abbey, A. F., Beardmore, A., Mukerjee, K., Short, A. D. T., Chincarini, G., Campana, S., Citterio, O., Moretti, A., Pagani, C., Tagliaferri, G., Giommi, P., Capalbi, M., Tamburelli, F., Angelini, L., Cusumano, G., Bräuninger, H. W., Burkert, W., & Hartner, G. D. 2005, *Space Science Reviews*, 120, 165
- Cooper, T., Africa, S., Aguiar, J. G. D. S., & Linnolt, M. 2005, *IAU Circ.*, 8575, 2
- Della Valle, M., & Livio, M. 1995, *ApJ*, 452, 704
- Dennefeld, M., Riquebourg, F., & Damerdj, Y. 2005, *IAUC*, 8544, 1
- Drake, J. J., Wagner, R. M., Starrfield, S., Butt, Y., Krautter, J., Bond, H. E., Della Valle, M., Gehrz, R. D., Woodward, C. E., Evans, A., Orio, M., Hauschildt, P., Hernanz, M., Mukai, K., & Truran, J. W. 2003, *ApJ*, 584, 448
- Ederoclite, A., Mason, E., dall, T. H., & Liller, W. 2005, *IAUC*, 8497, 2
- Ferland, G.J., Korista, K.T., Verner, D.A., Ferguson, J.W., Kingdon, J.B. & Verner, E.M. 1998, *PASP*, 110, 761
- Fujii, M., & Yamaoka, H. 2005, *IAU Circ.*, 8617, 3
- Gallagher, J. S., & Starrfield, S. 1978, *ARAA*, 16, 171
- Gilmore, A. C., & Kilmartin, P. M. 2005, *IAUC*, 8559, 2
- Gonzalez-Riestra, R., Shore, S. N., Starrfield, S., & Krautter, J. 1996, *IAU Circ*, 6295, 1
- Greiner, J., Orio, M., & Schartel, N. 2003, *A&A*, 405, 703
— 2003b, *A&A*, 405, 703
- Haseda, K., West, D., Yamaoka, H., & Masi, G. 2002, in *IAU Circular*, Vol. 7975, 1
- Heywood, I., O'Brien, T. J., Eyres, S. P. S., Bode, M. F., & Davis, R. J. 2005, *MNRAS*, 362, 469
- Hirosawa, K., Yamamoto, M., Nakano, S., Kojima, T., Iida, M., Sugie, A., Takahashi, S., & Williams, G. V. 1995, *IAU Circ.*, 6213, 1
- Iijima, T., Rosino, L., & Della Valle, M. 1998, *A&A*, 338, 1006
- Iijima, T., & Esenoglu, H. H. 2003, *A&A*, 404, 997
- Kiss, L., Bessel, M., & Retter, A. 2005, *IAUC*, 8612, 2
- Kiss, L. L., & Thomson, J. R. 2000, *A&A*, 355, L9
- Krautter, J., Ögelmann H., Starrfield S., Wichmann R., Pfeffermann E. 1996, *ApJ* 456, 788
- Krautter, J., & Williams, R. E. 1989, *ApJ*, 341, 968
- Lane, B. F., Retter, A., Eisner, J. A., Thompson, R. R., & Muterspaugh, M. W., 2006, "Interferometric Observations of Explosive Variables: V838 Mon, Nova Aql 2005 & RS Oph," in "Interferometry for Optical Astronomy," eds., Proceedings of SPIE (the International Society of Photo-optical Instrumentation Engineers), 6268-161
- Lanz, T., Telis, G. A., Audard, M., Paelers, F., Rasmussen, A. P., & Hubeny, I. 2005, *ApJ*, 619, 517
- Liller, W. 2005a, *IAUC*, 8497, 1
- Liller, W. 2005b, *IAUC*, 8559, 1
- Liller, W. 2005c, *IAUC*, 8596, 1
- Liller, W. 2005d, *IAUC*, 8635, 1
- Lyke, J. E., Kelley, M. S., Gehrz, R. D., & Woodward, C. E. 2002, *Bulletin of the American Astronomical Society*, 34, 1161
- Mazuk, S., Lynch, D. K., Rudy, R. J., Venturini, C. C., Puetter, R. C., Perry, R. B., & Walp, B. 2005, *IAU Circ*, 8644, 1
- Moretti, A., Campana, S., Tagliaferri, G., Abbey, A. F., Ambrosi, R. M., Angelini, L., Beardmore, A. P., Bräuninger, H. W., Burkert, W., Burrows, D. N., Capalbi, M., Chincarini, G., Citterio, O., Cusumano, G., Freyberg, M. J., Giommi, P., Hartner, G. D., Hill, J. E., Mori, K., Morris, D. C., Mukerjee, K., Nousek, J. A., Osborne, J. P., Short, A. D. T., Tamburelli, F., Watson, D. J., & Wells, A. A. 2004, in *X-Ray and Gamma-Ray Instrumentation for Astronomy XIII*. Edited by Flanagan, Kathryn A.; Siegmund, Oswald H. W. Proceedings of the SPIE, Volume 5165, pp. 232-240 (2004)., ed. K. A. Flanagan & O. H. W. Siegmund, 232
- Mukai, K., & Ishida, M. 2001, *ApJ*, 551, 1024
- Munari, U., Goranskij, V. P., Popova, A. A., Shugarov, S. Y., Tatarnikov, A. M., Yudin, B. F., Karitskaya, E. A., Kusakin, A. V., Zwitter, T., Lepardo, A., Passuello, R., Sostero, G., Metlova, N. V., & Shenavrin, V. I. 1996, *A&A*, 315, 166
- Munari, U., Siviero, A., Navasardyan, H., & Dallaporta, S. 2006, *A&A*, 452, 567
- Munari, U., Henden, A., Pojmanski, G., Dallaporta, S., Siviero, A., & Navasardyan, H. 2006, *MNRAS*, 369, 1755
- Naito, H., Tokimasa, N., Yamaoka, H., & Fujii, M. 2005, *IAU Circ.*, 8576, 2
- Nakano, S., Tago, A., Sakurai, Y., Kushida, R., & Kadota, K. 2004, *IAUC*, 8443, 1
- Ness, J.-U., Starrfield, S., Burwitz, V., Wichmann, R., Hauschildt, P., Drake, J. J., Wagner, R. M., Bond, H. E., Krautter, J., Orio, M., Hernanz, M., Gehrz, R. D., Woodward, C. E., Butt, Y., Mukai, K., Balman, S., & Truran, J. W. 2003, *ApJL*, 594, L127
- Ness, J.-U., Starrfield, S., Jordan, C., Krautter, J., & Schmitt, J. H. M. M. 2005, *MNRAS*, 364, 1015
- Ness, J.-U., Starrfield, S., & Schwarz, G. 2006a, in *Proceedings of WORKSHOP High resolution X-ray spectroscopy: towards XEUS and Con-X (2006)*
- Ness, J.-U., Starrfield, S., Schwarz, G., Vanlandingham, K., Wagner, R. M., Lyke, J., Woodward, C. E., Lynch, D. K., & Krautter, J. 2006b, *IAU Circ*, 8676, 2
- Ness, J.-U., Starrfield, S., Schwarz, G., Vanlandingham, K., Wagner, R. M., Lyke, J., Woodward, C. E., Lynch, D. K., Krautter, J., & Schmitt, J. H. M. M. 2006c, *Central Bureau Electronic Telegrams*, 598, 1 (2006). Edited by Green, D. W. E., 598, 1
- Nielbock, M., & Schmidtobreck, L. 2003, *A&A*, 400, L5
- Orio, M., Parmar, A., Benjamin, R., et al. 2001a, *MNRAS*, 326, L13
- Orio, M., Covington, J., Ogelman, H. 2001b, *A&A*, 373, 542
- Orio, M., Hartmann, W., Still, M., & Greiner, J. 2003, *ApJ*, 594, 435
- Orio, M. 2004, in *Revista Mexicana de Astronomía y Astrofísica Conference Series*, ed. G. Tovmassian & E. Sion, Vol. 20 (Instituto de Astronomía, Universidad Nacional Autónoma de México), 182
- Osborne, J. P., Page, K. L., & Bode, M. 2006, *Science in prep*
- Paelers, F., Rasmussen, A. P., Hartmann, H. W., Heise, J., Brinkman, A. C., de Vries, C. P., & den Herder, J. W. 2001, *A&A*, 365, L308
- Pereira, A. 1999, *IAU Circ*, 7323, 1
- Perry, R. B., Venturini, C. C., Rudy, R. J., Mazuk, S., Lynch, D. K., Puetter, R. C., & Walp, B. 2005, *IAUC*, 8638, 1
- Pietsch, W., Fliri, J., Freyberg, M. J., Greiner, J., Haberl, F., Riffeser, A., & Sala, G. 2005, *A&A*, 442, 879
- Petz, A., Hauschildt, P. H., Ness, J.-U., & Starrfield, S. 2005, *A&A*, 431, 321
- Pietsch, W., Haberl, F., Sala, G., Stiele, H., Hornoch, K., Riffeser, A., Fliri, J., Bender, R., Buehler, S., Burwitz, V., Greiner, J., & Seitz, S. 2006, *ArXiv Astrophysics e-prints*
- Pojmanski, G., & Oksanen, A. 2005, *IAUC*, 8540, 1
- Pojmanski, G., Nakano, S., Nishimura, H., Hashimoto, N., & Urata, T. 2005a, *IAU Circ.*, 8574, 1
- Pojmanski, G., Yamaoka, H., Haseda, K., Puckett, T., Hornoch, K., Schmeer, P., & Samus, N. N. 2005b, *IAU Circ*, 8617, 1
- Puetter, R. C., Rudy, R. J., Lynch, D. K., Mazuk, S., Venturini, C. C., Perry, R. B., & Walp, B. 2005, *IAUC*, 8640, 2
- Rauch 1997, *A&A*, 320, 237
- Rudy, R. J., Lynch, D. K., Mazuk, S., Venturini, C. C., Puetter, R. C., Perry, R. B., & Walp, B. 2005, *IAU Circ*, 8643, 2
- Schwarz, G.J., Shore, S.N., Starrfield, S., Hauschildt, P.H., Della Valle, M., & Baron, E. 2001, *MNRAS*, 320, 103
- Schwarz, G.J., et al. 2007, *ApJ* in press
- Shore, S.N., Sonneborn, G., Starrfield, S., Gonzalez-Riestra, R., & Polidan, R.S. '994, *ApJ*, 421,344
- Shore, S. N., Schwarz, G., Bond, H. E., Downes, R. A., Starrfield, S., Evans, A., Gehrz, R. D., Hauschildt, P. H., Krautter, J., & Woodward, C. E. 2003, *AJ*, 125, 1507
- Sitko, M. L., Kimes, R., Lynch, D. K., Russell, R. W., Kim, D. L., & Griep, D. 2005, *IAU Circ.*, 8575, 1
- Siviero, A., Munari, U., & Jones, A. F. 2005, *Informational Bulletin on Variable Stars*, 5638, 1
- Starrfield, S. 1991 in *Variability in Stars and Galaxies* (Bamberg, Germany)
- Starrfield, S., Shore, S. N., Butt, Y., Drake, J., Bond, H. E., Downes, R., Krautter, J., Wagner, R. M., Gehrz, R. D., Woodward, C. E., Della Valle, M., Hauschildt, P. H., & Truran, J. W. 2000, *Bulletin of the American Astronomical Society*, 32, 1253

Soma, M., Takao, A., Yamaoka, H., Haseda, K., Gilmore, A. C.,
 Kilmartin, P. M., Nakano, S., & Kadota, K. 2005, IAUC, 8607,
 1
 van den Bergh, S., & Younger, P. F. 1987, A&AS, 70, 125

Walter, F. M., Bond, H. E., & Pasten, A. 2005, IAU Circ., 8576, 3

APPENDIX

A. APPENDIX

A.1. *Targets*

In this section we summarize some background information of our targets in addition to that given in Table 1, collected mostly from unreferenced literature and private communications.

A.1.1. *V574 Pup*

V574Pup was independently discovered by Tago and Sakurai (Nakano et al. 2004). The evolution of its early light curve and spectral energy distribution is provided in Siviero et al. (2005). The FWHM of $H\alpha$ in the early spectrum was 650 km s^{-1} but with P-Cygni absorption extending to 860 km s^{-1} . Based on the intrinsic colors of the nova both at maximum and at t_2 , the same authors derived an extremely low reddening value of $E(B-V) \sim 0.05$. However, this value seems too low due to the low galactic latitude ($b \sim 2^\circ$) and the distance ($\sim 3.5 \text{ kpc}$) of this nova. Optical and near-IR spectra obtained one year after outburst showed that V574Pup had entered a coronal phase with lines of [S VIII], [S IX], [Si VI], [Si VII], and [Ca VIII] (Rudy et al. 2005). Analysis of the ratio of the O I lines in this data set and those obtained later implies a higher reddening of $E(B-V) = 1.27$ (Rudy, private communication).

A.1.2. *V382 Nor*

V382Nor was discovered prior to visual maximum on 13.3 Mar, 2005 (Liller 2005a). Examining the AAVSO light curve, visual maximum probably occurred on 19 March, 2005 at $V \sim 9$. The B-V color obtained on 20 March was 0.8 ± 0.11 (Liller 2005a), which gives an $E(B-V)$ of 0.57 ± 0.17 based on the intrinsic color at maximum ($B-V = +0.23 \pm 0.06$; van den Bergh & Younger 1987). Another determination of the reddening uses the intrinsic (B-V) color at t_2 , -0.02 ± 0.04 (van den Bergh & Younger 1987). The (B-V) color at t_2 was ~ 1.1 , which implies $E(B-V) \sim 1.1$. This high a reddening estimate is supported by the saturated Na I interstellar lines in the spectra taken at the same time (Ederoclite et al. 2005). The P-Cygni profiles seen in the early spectra imply an average expansion velocity of 1100 km s^{-1} .

A.1.3. *V1663 Aql*

V1663 Aql was discovered on 9.2 June, 2005 during routine All Sky Automated Survey patrols (Pojmanski & Oksanen 2005). Spectroscopy obtained one day after maximum showed an extremely red continuum implying significant reddening toward the source (Dennefeld et al. 2005). The emission lines had narrow P-Cygni profiles with expansion velocities of order 700 km s^{-1} . By 14 November V1663 Aql had entered its nebular phase with [O III] in the optical and the coronal lines of [S VIII], [S IX], [Si VI] and [Si VII] present in the near-IR (Puetter et al. 2005). The expansion velocity, as measured from the FWHM of the emission lines, was 2000 km s^{-1} (Puetter et al. 2005). The ratio of the O I lines also confirmed the large extinction, with a value as large as $E(B-V) = 2$ (Puetter et al. 2005). Lane et al. (2006) reported an angular expansion of 0.2 mas/day at $2.2 \mu\text{m}$ with the Palomar Testbed Interferometer. This corresponds to a distance of $5.5 \pm 1 \text{ kpc}$ assuming expansion velocities between $700 - 1000 \text{ km s}^{-1}$. If the expansion velocities are larger, as measured by Puetter et al. (2005), then the distance must also be larger than that derived by Lane et al. (2006).

A.1.4. *V5116 Sgr*

On 4 July, 2005 Liller discovered V5116 Sgr already on the decline. His first observations implied that visual maximum was brighter than 8 mag (Liller 2005b). The P-Cygni line profile of $H\alpha$ suggested an expansion velocity of 1300 km s^{-1} from spectra taken a day after discovery (Gilmore & Kilmartin 2005). They also reported a B-V color of $+0.47 \pm 0.02$ on 5 July. Using the intrinsic (B-V) color at maximum for V5116 Sgr implies an $E(B-V) = 0.24 \pm 0.08$.

A.1.5. *V1188 Sco*

V1188 Sco was discovered in late July 2005 (Pojmanski et al. 2005a). The visual maximum was measured by Cooper et al. (2005). The only spectral information in the literature was obtained within days after visual maximum. Optical spectra were consistent with a typical CO type nova with broad $H\alpha$, FWHM and Full Width at Zero Intensity (FWZI) of 1730 and 4000 km s^{-1} , and Fe II P-Cyg emission lines (Naito et al. 2005; Walter et al. 2005). A 3 - 14 micron spectrum taken one day after visual maximum displayed a featureless continuum consistent with the Rayleigh-Jeans tail of the Planck function (Sitko et al. 2005). The Na I D line was observed with three absorption components and an equivalent width of 0.5 nm (Walter et al. 2005) implying a large extinction.

A.1.6. *V1047 Cen*

Little is known about V1047Cen due to its extreme southern declination ($> -62^\circ$). It was discovered by Liller (2005c) on 1.031 September, 2005. Visual maximum probably occurred three days later at $V = 8.83$ but there is very

little reported data on the early light curve, so its subsequent behavior, including its t_2 decay time, is unknown. The spectrum at maximum resembled that of V5114 Sgr and V5116 Sgr with an $H\alpha$ FWHM of $840 \pm 50 \text{ km s}^{-1}$ (Liller 2005c).

A.1.7. V476 Sct

V476 Sct was discovered after visual maximum on 30.5 Sept, 2005 by A. Takao (Soma et al. 2005). Haseda (2005) reported an independent discovery on the same day with a visual magnitude of 10.9. Early optical spectra showed many emission lines, notably of Fe II (Munari et al. 2006b). In the spectra the prominent lines showed double-peak profiles with velocity separations of $\sim 700 \text{ km s}^{-1}$ and FWHM of order 1000 km s^{-1} . Optical and near-IR spectra obtained six weeks after maximum showed similar emission features but with a strong red continuum implying the presence of a dust shell in the ejecta. The reddening inferred from the ratio of the O I lines at that time was $E(B-V) \sim 2$ (Perry et al. 2005). This value is similar to that derived by Munari et al. (2006b) using the color evolution and strength of the diffuse 6614 \AA interstellar band.

A.1.8. V477 Sct

The second nova discovered in the constellation Scutum in 2005, V477 Sct, was detected independently by G. Pojmanski and K. Haseda on images obtained on the 11th and 13th of October, 2005, respectively, and the maximum visual magnitude was recorded on 13.07 October at $V = 10.44 \text{ mag}$ (Pojmanski et al. 2005b). Early *JHK* spectroscopy of V477 Sct showed broad H I emission lines with FWZI of 6000 km s^{-1} and no evidence of dust emission (Pojmanski et al. 2005b). Optical spectra confirmed broad emission lines with a FWHM value of $H\alpha = 2900 \text{ km s}^{-1}$ (Fujii & Yamaoka 2005). The optical spectra of Munari et al. (2006a) showed that unlike V476 Sct which was rich in Fe II lines, V477 Sct had He and N lines. Although sparse, the light curve revealed a rapid decline with an estimated t_2 of only 3 days (Munari et al. 2006a). This rapid decline was consistent with the large expansion velocities. Optical and near-IR spectra taken on 15.094 November, 2005 showed a continuum increasing toward the red, possibly due to thermal dust emission (Mazuk et al. 2005). Numerous emission lines were observed which had developed double peak profiles with a FWHM of 2700 km s^{-1} . The features present included the coronal lines [S VII] and [S IX] but not [Ca VII] or [Si VI]. The ratio of the O I lines implied a substantial reddening of $E(B-V) = 1.2$ (Mazuk et al. 2005). A similar value of ≥ 1.3 was determined by Munari et al. (2006a) based on the early color evolution, extinction maps along the line of sight, and the large equivalent width of the diffuse interstellar band at 6614 \AA .

A.1.9. LMC 2005

Liller discovered LMC 2005 on 26.16 November 2005, but it was also present on images that he had taken four days earlier. Visual maximum occurred 27 November at $V = 12.6 \text{ mag}$ (Liller 2005d). The light curve evolution was extremely slow and in early 2006 exhibited photometric evidence of dust formation (F. Walter, private communication).

A.1.10. V723 Cas

V723 Cas is a slow nova. It was discovered on 24 August, 1995 by Yamamoto (Hirosawa et al. 1995) at $V = 9.2 \text{ mag}$. Prediscovery observations showed that it had slowly brightened over the previous 20 days. The subsequent light curve was unusual. V723 Cas reached a maximum magnitude of $V \sim 8.6 \text{ mag}$ one hundred days after discovery. At that point V723 Cas exhibited a flare to 7.1 mag on 17 December, 1995. During the flare the $U - B$ colors became significantly bluer while the $B - V$ color remained constant (Munari et al. 1996). The light curve also had additional secondary flares during the following 400 days. V723 Cas has been extensively observed from the ultraviolet (Gonzalez-Riestra et al. 1996) to radio (Heywood et al. 2005) wavelengths. Recent optical and NIR spectra showed that V723 Cas reached a "coronal" phase with emission from high ionization stages such as [Fe X] (6373 \AA) similar to spectra obtained of GQ Mus in the late 1980s (Krautter & Williams 1989). The spectral similarity suggests ongoing nuclear burning on the WD (Krautter & Williams 1989). As a result, we requested *Swift* observations in order to search for the X-ray emission that would be related to ongoing nuclear burning.

A.1.11. V1494 Aql

V1494 Aql was discovered on 1.8 December, 1999 at $V = 6.0 \text{ mag}$ by Pereira (1999). Within a few days of discovery this nova reached a peak magnitude exceeding 4. It subsequently declined by two magnitudes in 6.6 ± 0.5 days thus classifying V1494 Aql as a fast nova (Kiss & Thomson 2000). Three *Chandra* ACIS-I observations were carried spectrum with no obvious soft component. However, a bright SSS spectrum was present in the August spectrum (Starrfield et al. 2000). One month later, two grating observations were obtained on 28 September and 1 October, 2000, which showed remarkable variability (Drake et al. 2003). The spectrum resembles that of the SSS Cal 83 (Paerels et al. 2001), except that it appeared somewhat hotter and the "emission features" were at different wavelengths. A final observation with *Chandra* LETGS one year later (ObsID 2681) showed no emission in the dispersed spectrum but a reasonable detection in the zeroth order on the HRC-S detector. We extracted 56 counts on a background of 10, corresponding to a count rate of 2 cts/ksec and a $14\text{-}\sigma$ detection likelihood. Unfortunately, the HRC detector does not provide the energy resolution to construct a spectrum.

A.1.12. *V4743 Sgr*

V4743 Sgr was discovered by Haseda et al. (2002). A distance of 6.3 kpc is assumed based on infrared observations (Lyke et al. 2002). *Chandra* grating observations were carried out on 19 March, 2003 (Ness et al. 2003). The light curve showed large amplitude oscillations ($\sim 20\%$ of the count rate) with a period of 1324 sec (almost 40% power) with the 2nd and 3rd harmonic overtones present. V4743 Sgr was observed by *Chandra* on five more dates and details of the spectral evolution will be presented by Ness et al. (in prep).

A.2. *Extraction of source counts*

In this section we give a detailed account of our methods to determine the count rates and detection probabilities. We determined the positions of the sources on the chip from the individual sky coordinates and used circular extraction regions (radius 10 pixels = 23.6", which encircles $\sim 80.5\%$ of the total PSF). For the extraction of the background we defined annular extraction regions around the source position with an inner radius of 10 pixels and an outer radius of 100 pixels. We carefully checked to make sure that no sources were present in the background extraction regions. We scaled the number of extracted background counts by the ratio of extraction regions (99.0) to determine the number of expected background counts per detect cell. We assume Poissonian noise and thus apply a maximum likelihood estimation in order to determine the net source count rate. We define two model parameters S and B that represent the number of expected counts of source and background for the source extraction region and calculate the number of expected counts in the source- and background extraction regions N_s and N_b :

$$N_s = \alpha S + B \quad N_b = (1 - \alpha)S + \beta B \quad (\text{A1})$$

with $\alpha = 0.80$ the fraction of the PSF included in the detect cell and $\beta = 99$ the ratio of background- to source extraction areas. Under the assumption of Poissonian statistics we can calculate the probability of finding the measured numbers of counts n_s and n_b in the respective extraction regions when S and B are given:

$$P = \frac{N_s^{n_s}}{n_s!} e^{-N_s} \frac{N_b^{n_b}}{n_b!} e^{-N_b} \quad (\text{A2})$$

and thus the likelihood can be calculated

$$\mathcal{L} = -2 \ln P = -2n_s \ln(\alpha S + B) - (\alpha S + B) + n_b \ln((1 - \alpha)S + \beta B) - ((1 - \alpha)S + \beta B) + \text{const}. \quad (\text{A3})$$

We seek solutions for S and B where \mathcal{L} reaches a minimum, which holds for $N_s = n_s$ and $N_b = n_b$, and thus

$$S = \frac{n_b - \beta n_s}{1 - \alpha - \alpha\beta}, \quad B = \frac{n_s - \alpha(n_s + n_b)}{1 - \alpha - \alpha\beta} \quad (\text{A4})$$

leading to a minimum value \mathcal{L}_{\min} of

$$\mathcal{L}_{\min} = -2[n_s(\ln n_s - 1) + n_b(\ln n_b - 1)]. \quad (\text{A5})$$

With the definition of \mathcal{L} the range between \mathcal{L}_{\min} and $\mathcal{L}_{\min} + 1$ is equivalent to the 68.3-percent uncertainty range of the critical parameter S . We thus obtained the formal 1- σ errors by varying S until the value of \mathcal{L} had increased by 1.0 from the minimum while leaving B fixed at the value obtained from Eq. A4.

The value of \mathcal{L}_{\min} can also be used to calculate the detection probability (in percent) based on the likelihood ratio test, which is a statistical test of the goodness-of-fit between two models. A relatively more complex model is compared to a simpler model (null hypothesis) to see if it fits a particular dataset significantly better. We define the likelihood for the null hypothesis \mathcal{L}_0 as $\mathcal{L}(S = 0)$, and

$$\Delta\mathcal{L} = \mathcal{L}(S) - \mathcal{L}_0 \quad (\text{A6})$$

quantifies the improvement in \mathcal{L} after including $S > 0$. The parameter B is an "uninteresting parameter" as defined by Avni (1976), and we thus convert $\Delta\mathcal{L}$ to the probability for *one* degree of freedom using the IDL¹⁰ function `chisqr_pdf`.

In cases where no counts were found in the detect cell ($n_s = 0$), or when the number of counts in the detect cell is smaller than that expected from the background ($n_s < n_b$), we calculated the 95-percent upper limits from the number of expected background counts and those actually measured in the detect cell. We again used the likelihood ratio test and solved Eq. A6 for $\mathcal{L}(S)$ according to Eq. A3 yielding the value of S that returns $\Delta\mathcal{L} = 4$. We also calculated upper limits in cases where the derived 1- σ uncertainties were larger than the measured count rate.

In addition to the formal detection likelihood we consider whether the photons inside the source extraction region show some concentration towards the center, and whether their energy distribution is different from that of the instrumental background. In order to assess the concentration towards the center, we give the percentage of counts that we found in the central quarter of the detect cell in the last column of Table 2. From the PSF we expect 60.5 percent of source photons to be within a circle of radius 5 pixels, and any number much below this fraction is likely not a source. We also studied the spectral energy distribution of the background compared to that of the source as an auxiliary criterion. We computed the median of recorded energies of the source counts and compared with

¹⁰ Interactive Data Language, ITT Corporation

the same value from the background. These values are marked by vertical lines (gray dotted for background and black dashed for source in Figs. 3 to 11). In order to assess the probability that the background spectrum is softer than the source spectrum, we generated 1000 spectra with n_s counts drawn as random sub-samples out of the pool of extracted background counts n_b and calculated the median value for each generated spectrum. While a situation in which 50 percent of all random cases returned lower median energies does not imply a non-detection, any strong deviation from 50 percent is supportive of an independent source spectrum.